

CONNECTING STRUCTURE FUNCTIONS ON THE LATTICE WITH PHENOMENOLOGY

W. DETMOLD¹, W. MELNITCHOUK², A. W. THOMAS¹

¹ *Special Research Centre for the Subatomic Structure of Matter, and Department of Physics
 and Mathematical Physics, Adelaide University 5005, Australia*

² *Jefferson Lab, 12000 Jefferson Avenue, Newport News, Virginia 23606, USA*

We examine the extraction of moments of parton distributions from lattice data, focusing in particular on the chiral extrapolation as a function of the quark mass. Inclusion of the correct chiral behavior of the spin-averaged isovector distribution resolves a long-standing discrepancy between the lattice moments and experiment. We extract the x -dependence of the valence $u - d$ distribution from the lowest few lattice moments, and discuss the implications for the quark mass dependence of meson masses lying on the ρ Regge trajectory. The role of chiral symmetry in spin-dependent distributions, and in particular the lattice axial vector charge, g_A , is also highlighted.

1. Introduction

Parton distribution functions (PDFs) parameterize fundamental information on the nonperturbative structure of the nucleon, and the workings of QCD at low energy. Over the past two decades considerable experience has been gained with studies of PDFs within low energy models of the nucleon. Ultimately, however, one would like a more rigorous connection of PDFs with QCD, and presently this can only be provided through the lattice formulation of QCD.

Because PDFs are defined as light cone correlation functions, it is not possible to calculate them directly on the lattice in Euclidean space. Instead, one calculates matrix elements of local twist-two operators, which are related through the operator product expansion to moments of the PDFs. For the spin-averaged quark distributions, $q(x) = q^\uparrow(x) + q^\downarrow(x)$, the moments are defined as:

$$\langle x^n \rangle_q = \int_0^1 dx x^n (q(x) + (-1)^{n+1} \bar{q}(x)) , \quad (1)$$

while moments of the helicity distributions, $\Delta q(x) = q^\uparrow(x) - q^\downarrow(x)$, are given by:

$$\langle \Delta x^n \rangle_q = \int_0^1 dx x^n (\Delta q(x) + (-1)^n \Delta \bar{q}(x)) . \quad (2)$$

A number of lattice calculations of PDF moments have been performed over the last decade, initially in the quenched approximation, and more recently with dynamical quarks. The results indicate that at the relatively large quark masses at which the

calculations were made (between $m_q \approx 30$ and 190 MeV), the unquenched results are indistinguishable from the quenched within the current errors.

Despite the impressive progress of the lattice calculations, for many years the moments $\langle x^n \rangle_q$ have yielded results which were typically $\sim 50\%$ larger than the experimental values, when linearly extrapolated to the physical quark masses. This discrepancy was recently resolved with the observation¹ that a linear extrapolation in quark mass omits crucial physics associated with the nucleon's pion cloud, and that inclusion of the nonanalytic dependence on the quark mass is essential if one is to reconcile the lattice data with experiment.

In this paper we report recent progress made in connecting moments of parton distributions calculated on the lattice with experiment, focusing on the extraction of the $u - d$ moments (which are insensitive to the poorly known disconnected contributions¹). We discuss the extraction of the x dependence from moments, and the implications for masses of mesons lying on the ρ Regge trajectory, and outline the role of chiral symmetry in helicity distributions and the axial vector charge, g_A .

2. Chiral Extrapolation of Lattice Moments

The spontaneous breaking of the chiral $SU(2)_L \times SU(2)_R$ symmetry of QCD generates the nearly massless Goldstone bosons (pions), whose importance in hadron structure is well documented. At small pion masses, PDF moments can be systematically expanded in a series in m_π , with the expansion coefficients generally free parameters. One of the unique consequences of pion loops, however, is the appearance of terms nonanalytic in the quark mass, $m_q \propto m_\pi^2$, which arise from the infrared behavior of the chiral loops, and are therefore model independent.

The leading order (in m_π) nonanalytic term in the expansion of the moments of PDFs was shown by Thomas et al.² to have the generic behavior $m_\pi^2 \log m_\pi$. On the other hand, in the heavy quark limit, in which the valence quark distributions become δ -functions centered at $x = 1/3$, the moments $\langle x^n \rangle_{u-d}$ approach $1/3^n$. An extrapolation formula which explicitly satisfies both the heavy quark and chiral limits can be written:³

$$\langle x^n \rangle_{u-d} = a_n \left(1 + c_{\text{LNA}} m_\pi^2 \log \frac{m_\pi^2}{m_\pi^2 + \mu^2} \right) + b_n \frac{m_\pi^2}{m_\pi^2 + \lambda_n^2}, \quad (3)$$

in which the coefficient of the leading nonanalytic (LNA) term, $c_{\text{LNA}} = -(1 + 3g_A^2)/(4\pi f_\pi)^2$, is calculated from chiral perturbation theory.^{4,5} The mass μ reflects the scale at which the Compton wavelength of the pion becomes comparable to the size of the hadron (without its pion cloud). Previous fits¹ to the lattice moments of $u-d$ suggest a value $\mu \approx 550$ MeV, which is consistent with values found⁶ in analyses of nucleon static properties. The b_n term in Eq. (3), $b_n = 1/3^n - a_n (1 - \mu^2 c_{\text{LNA}})$, is included in order to provide a linear dependence on m_π^2 , and the mass scale λ_n is set to be 5 GeV for all n .

In Fig. 1 we show the best χ^2 fit to the lattice data^{7,8} for the $n = 1$ moment of $u - d$ as a function of m_π^2 . Clearly, an extrapolation based on Eq. (3) provides a

much better fit to the lattice data and experiment than a linear fit. Similar results are found¹ for the $n = 2$ and $n = 3$ moments. Unfortunately, because all of the lattice data are in a region where the moments show little variation with m_π^2 , it is not possible to determine μ from the current data, and within the errors both the lattice data and the experimental values can be fitted with μ ranging from ~ 400 to 700 MeV. Data at smaller quark masses are therefore crucial to constrain this parameter and guide an accurate extrapolation.

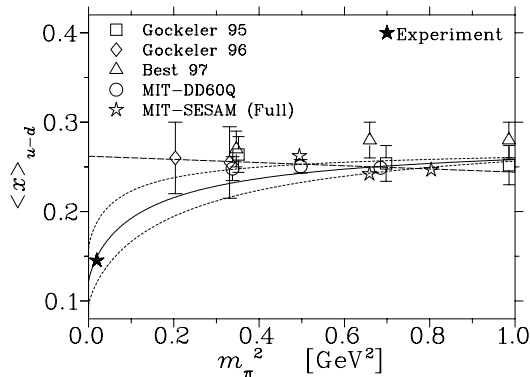


Fig. 1. The $n = 1$ moment of the $u - d$ distribution, with a best fit to data^{7,8} using Eq.(3) with $\mu = 550$ MeV (solid), and $\mu = 400$ and 700 MeV (upper and lower dotted), compared with a linear extrapolation (dashed).

3. Quark Distributions from Lattice Moments

Having established the appropriate way to extrapolate lattice data on PDF moments, one can now ask much information can the existing data provide on the x dependence of the PDFs. The reconstruction of the complete x dependence in principle requires infinitely many moments, however, on the lattice, because of operator mixing for operators with spin ≥ 5 , all calculations have so far been restricted to $n \leq 3$. Nevertheless, as shown by Detmold et al.,³ considerable information on the shape of the valence $u_v - d_v$ distribution can already be inferred from just the lowest four moments.

The most efficient way to reconstruct the PDF from a limited number of moments is to determine the parameters of the PDF parameterization by directly fitting to the moments. For the isovector valence distribution accurate PDFs can be reconstructed from the lowest four moments, using the standard parameterization,

$$xq_v(x) \equiv x(q(x) - \bar{q}(x)) = \alpha x^\beta (1-x)^\delta (1 + \epsilon\sqrt{x} + \gamma x), \quad (4)$$

where β can be related through Regge theory to the intercept of the ρ Regge trajectory, and δ is given by perturbative QCD counting rules.

Note that some care must be taken when attempting to extract information on valence quark distributions from both the even and odd moments. While the even n moments of $u - d$ correspond to the valence distribution, $u_v - d_v$, the odd n moments correspond to the combination $u_v - d_v + 2\bar{u} - 2\bar{d}$. The difference between these represents the famous violation of the Gottfried sum rule. Given sufficiently many moments of $u - d$, one can reconstruct both the valence $u_v - d_v$ and $\bar{u} - \bar{d}$ distributions by fitting the even and odd moments separately. However, at present there exists only a single data point for the even moments, $n = 2$ (the $n = 0$ point corresponds to normalization), which makes it difficult to obtain accurate information. To minimize the error associated with reconstruction of the $\bar{u} - \bar{d}$ distribution, we subtract the values of the phenomenological moments of $\bar{d} - \bar{u}$ from the calculated odd moments. The correction to the $n = 1$ moment is $< 10\%$, while for $n = 3$ it is a fraction of a percent.

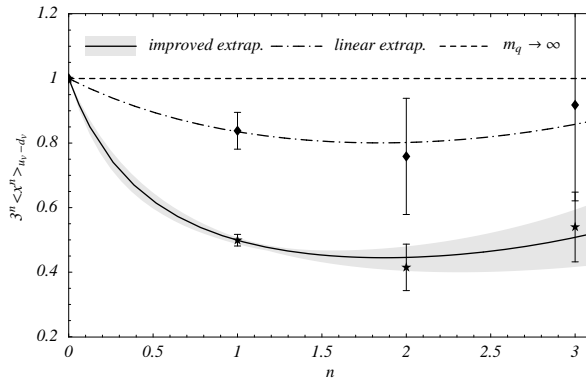


Fig. 2. Moments of the valence $u_v - d_v$ distribution (scaled by 3^n) at the physical quark mass, extracted from fits to lattice data using a linear extrapolation (diamonds) and Eq. (3) (stars).

The resulting fits to the moments of the valence $u_v - d_v$ distribution are displayed in Fig. 2 for both the linear and improved extrapolation, Eq. (3), with the shaded region around the latter corresponding to a 1σ variation of the fit parameters from their optimal values. For clarity we plot 3^n times the moments, so that the horizontal line at unity represents the heavy quark limit.

The corresponding distributions $x(u_v - d_v)$ are displayed in Fig. 3. Once again, the lightly shaded region represents a 1σ deviation from the central values, while the darker band illustrates the spread between global PDF fits. A comparison of the distribution reconstructed using the improved chiral extrapolation with the phenomenological distributions shows reasonably good agreement. On the other hand, the linear extrapolation gives a distribution (scaled by a factor 1/2 in the figure) which has a significantly higher peak, centered at $x \sim 1/3$, reminiscent of a heavy, constituent quark-like distribution.

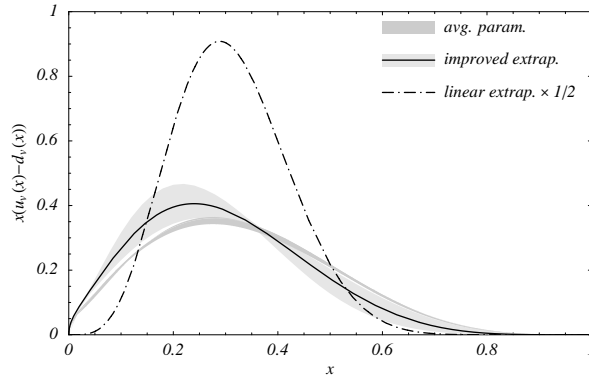


Fig. 3. Physical valence $x(u_v - d_v)$ distribution, extracted using Eq. (3) (solid), and a linear extrapolation, scaled by a factor $1/2$ (dot-dashed).

4. Regge Behavior and the ρ Regge Trajectory

According to Regge theory, the exponent β which governs the small- x behavior of the distribution $u_v - d_v$ is related to the intercept ($\approx 1/2$) of the isovector, C -odd, ρ Regge trajectory, and indeed the best fit³ to parameterizations of global data gives $\beta \approx 0.48$. The dependence of β on the quark mass obtained from the fits to moments in Sec. 3 therefore allows one to predict the m_q dependence of the Regge intercept.

In addition to the intercept, one also needs to determine the slope of the trajectory as a function of m_q . In the infinite mass limit, orbital excitations of mesons become energetically degenerate with the $L = 0$ state. Within Regge theory, this is possible only if $\beta \rightarrow \infty$ as $m_q \rightarrow \infty$, which is consistent with the valence distribution approaching a δ -function. One expects, therefore, that the slope should increase as m_q increases from its physical value. Using the lattice data for the ρ meson and the values of β generated from the fits in Fig. 2, one can then make predictions for the behavior of the masses of the orbital excitations as a function of m_q .

In Fig. 4 we show the predicted ρ Regge trajectory at $m_\pi = 0.785$ GeV, corresponding to the strange quark mass, compared with the trajectory at the physical light quark mass. A fit through the central values of β and the ρ mass⁹ at $m_\pi = 0.785$ GeV yields a slope which is larger than that of the trajectory at the physical quark mass, consistent with the expected trend towards the heavy quark limit.

Although lattice data for the masses of orbital excitations are scarce, there have been some pioneering calculations of the a_2 and ρ_3 meson masses by the UKQCD Collaboration,⁹ indicated by the filled boxes in Fig. 4 (we use the fact that the a_2 trajectory lies on top of the ρ trajectory). Comparing with the predictions from the PDF analysis, the calculated ρ_3 meson mass lies within the predicted band,

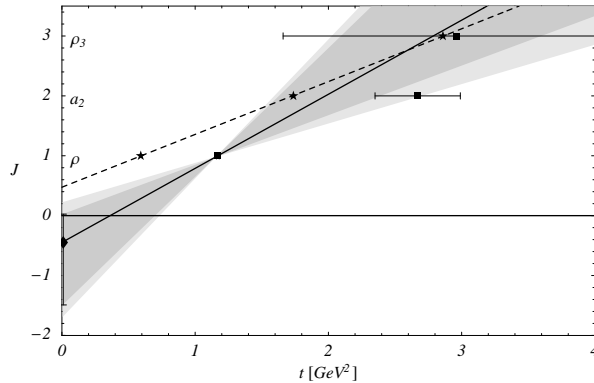


Fig. 4. Regge plot of the spin, J , versus $t = (\text{mass})^2$ of mesons on the ρ trajectory, at the physical pion mass (dashed) and at $m_\pi = 0.785 \text{ GeV}$ (solid). The physical masses of the ρ , a_2 and ρ_3 mesons are indicated by stars, while the boxes represent lattice masses.⁹ The darker shaded region represents the statistical error in the extrapolation, while the lighter region indicates an estimate of the systematic error associated with the fitting procedure.³

albeit within large errors, while the a_2 mass lies on the edge of the predicted range. Needless to say, further exploration of the masses of excited mesons within lattice QCD would be very helpful in testing these predictions.

5. Helicity Distributions

Lattice simulations of the spin-averaged quark distributions provide one of the benchmark calculations of hadron structure in lattice QCD. Having established confidence in the reliability of the lattice calculations through the correct treatment of the chiral behavior of the moments, we can now turn to other PDFs of the nucleon. Of particular importance are the helicity distributions, $\Delta q(x)$, which describe the distribution of the nucleon spin amongst its quark constituents.

While a complete determination of the helicity distributions requires calculation of the singlet distribution, $\Sigma_q \Delta q$, for which there have only been exploratory lattice calculations,^{10,11} a more basic challenge remains to understand the axial vector charge, g_A , given by the $n = 0$ moment of the isovector $u-d$ distribution. The results of several lattice calculations^{7,8,11} of g_A are compiled in Fig. 5. (Not included are results from recent simulations using domain wall fermions,¹² which appear to have strong finite volume dependence – see below.) When extrapolated linearly in m_q to the physical quark mass, the results are $\sim 10\text{--}15\%$ lower than the experimental value. Simulations with dynamical fermions⁸ (SESAM) yield results consistent with the earlier unquenched calculations^{7,8,11}.

On the other hand, the behavior of the moments $\langle \Delta x^n \rangle_{u-d}$ is known in the chiral⁵ and heavy quark limits, and can be used to constrain the extrapolation

form, as in Eq. (3):

$$\langle \Delta x^n \rangle_{u-d} = \tilde{a}_n \left(1 + \tilde{c}_{\text{LNA}} m_\pi^2 \log \frac{m_\pi^2}{m_\pi^2 + \mu^2} \right) + \tilde{b}_n \frac{m_\pi^2}{m_\pi^2 + \lambda_n^2}, \quad (5)$$

where $\tilde{c}_{\text{LNA}} = -(1 + 2g_A^2)/(4\pi f_\pi)^2$, and $\tilde{b}_n = 5/3^{n+1} - \tilde{a}_n(1 - \mu^2 \tilde{c}_{\text{LNA}})$. Using the same values of μ and λ_n as in Fig. 1, the results of the chiral extrapolation using Eq. (5) are shown in Fig. 5.

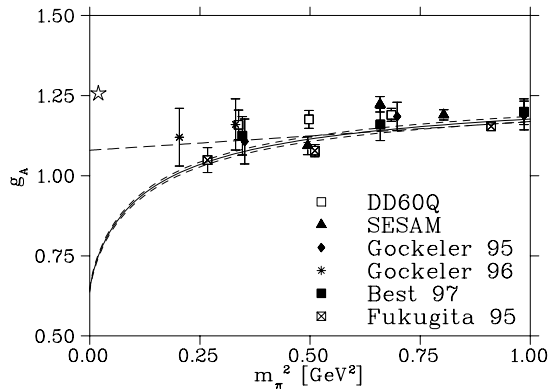


Fig. 5. Lattice data^{7,8,11} on the nucleon axial charge, g_A , extrapolated linearly in m_π^2 (long dashed), and using Eq. (5): best χ^2 fit (solid), and fits to extrema of error bars (short dashed).

The result for g_A is a downturn with decreasing m_q , making the discrepancy with the empirical value larger. The reasons for this could be severalfold. Firstly, the chiral behavior in Eq. (5) arises only from fluctuations $N \rightarrow \pi N \rightarrow N$, whereas it is well known that the Δ plays an important role in g_A through the fluctuation $N \rightarrow \pi\Delta \rightarrow N$. On the other hand, in the chiral limit the Δ has been shown⁵ to give vanishing chiral contributions at order $m_\pi^2 \log m_\pi$, suggesting that higher order effects in the chiral expansion are likely to be important. The inclusion of these effects is currently under investigation.

More importantly, perhaps, to fully incorporate the pion cloud in a lattice simulation a sufficiently large volume must be used. Indeed, there are some indications¹² of large finite volume effects for g_A , which tend to *increase* g_A in comparison with the results from smaller volumes. Clearly, in light of the results on the chiral extrapolation, it is imperative to perform simulations on larger lattices to understand the source of the discrepancy.

6. Conclusion

In this report we have highlighted the importance of model independent constraints from the chiral and heavy quark limits of QCD in the extrapolation of lattice data

on parton distribution moments. Inclusion of the nonanalytic structure associated with the infrared behavior of Goldstone boson loops leads to a resolution of a long-standing discrepancy between lattice data on low moments of the spin-averaged $u - d$ distribution and experiment.

The importance of ensuring the correct chiral behavior is further illustrated by comparing the x distributions obtained by extrapolating the lattice data using a linear and a chirally symmetric fit. While the latter gives an x distribution which is in quite good agreement with the phenomenological fits, the linearly extrapolated data give distributions with the wrong small- x behavior, which translates into a much more pronounced peak at $x \sim 1/3$, reminiscent of a heavy, constituent quark-like distribution. Our analysis suggests an intriguing connection between the small- x behavior of the valence distributions and the m_q dependence of meson masses on Regge trajectories, which should be tested more thoroughly in future simulations of the excited hadron spectrum.

Finally, we have highlighted the need for further study of moments of the helicity distributions, and the axial vector charge of the nucleon in particular, which appears to be underestimated in lattice simulations. The inclusion of the pion cloud of the nucleon leads to a larger discrepancy at the physical quark mass, indicating that lattice artifacts such as finite volume effects may not yet be under control. Further data on larger lattices, and at smaller quark masses, will be necessary to resolve this issue.

Acknowledgements

We are grateful to D.B. Leinweber, J.W. Negele and D.B. Renner for helpful discussions. This work was supported by the Australian Research Council, and the U.S. Department of Energy contract DE-AC05-84ER40150, under which the Southeastern Universities Research Association (SURA) operates the Thomas Jefferson National Accelerator Facility (Jefferson Lab).

References

1. W. Detmold, W. Melnitchouk, J. W. Negele, D. B. Renner and A. W. Thomas, *Phys. Rev. Lett.* **87**, 172001 (2001).
2. A.W. Thomas, W. Melnitchouk and F.M. Steffens, *Phys. Rev. Lett.* **85**, 2892 (2000).
3. W. Detmold, W. Melnitchouk and A.W. Thomas, *Eur. Phys. J. direct* **C 13**, 1 (2001).
4. D. Arndt and M.J. Savage, [nucl-th/0105045](#).
5. J.-W. Chen and X. Ji, [hep-ph/0105197](#); [hep-ph/0105296](#).
6. W. Detmold *et al.*, *Pramana* **57**, 251 (2001), [nucl-th/0104043](#).
7. M. Göckeler *et al.*, *Phys. Rev.* **D 53**, 2317 (1996); M. Göckeler *et al.*, *Nucl. Phys. Proc. Suppl.* **53**, 81 (1997); C. Best *et al.*, [hep-ph/9706502](#).
8. D. Dolgov *et al.*, *Nucl. Phys. Proc. Suppl.* **94**, 303 (2001).
9. P. Lacock, C. Michael, P. Boyle and P. Rowland, *Phys. Rev.* **D 54**, 6997 (1996).
10. S.J. Dong *et al.*, *Phys. Rev. Lett.* **75**, 2096 (1995); S. Güsken *et al.*, [hep-lat/9901009](#).
11. M. Fukugita *et al.*, *Phys. Rev. Lett.* **75**, 2092 (1995).
12. S. Sasaki, T. Blum, S. Ohta and K. Orginos, [hep-lat/0110053](#).